The status of GEO 600

S Hild (for the LIGO Scientific Collaboration)

Max-Planck-Institut für Gravitationsphysik (Albert-Einstein-Institut) und Universität Hannover, Callinstr. 38, D-30167 Hannover, Germany

E-mail: stefan.hild@aei.mpg.de

Abstract
The GEO 600 gravitational wave detector located near Hannover in Germany is part of an international network of gravitational wave observatories. As more and more of these detectors approach their final configuration, the focus is shifted from commissioning to detector characterization. At the moment, GEO 600, the first detector using advanced technologies such as dual recycling, is preparing for a long data-taking period starting at the beginning of summer 2006. In this paper, we give an overview of detector commissioning and the detector characterization work of GEO 600 for the period between March 2005 and February 2006.

PACS numbers: 04.80.Nn, 95.75.Kk

(Some figures in this article are in colour only in the electronic version)

1. Introduction

During the last decade, four large-scale laser-interferometric gravitational wave projects, LIGO [1], VIRGO [2], TAMA 300 [3] and GEO 600 [4], have been constructed and most of them are approaching their final detector configuration. This paper describes some highlights of the commissioning and detector characterization work of GEO 600 for a period between March 2005 and February 2006.

Figure 1 shows a simplified optical layout of the GEO 600 detector. The light of a 12 W master-slave laser system is injected into two sequential mode cleaners MC 1 and MC 2 of 8 and 8.1 m round-trip length and a finesse of 2700 and 1700, respectively. The stabilized and filtered light enters the main Michelson interferometer through the power-recycling mirror (MPR). The main interferometer consists of five optical components: the beam splitter (BS), two end mirrors (MCe and MCn) and two folding mirrors (MFe and MFn). In contrast to most of the other large-scale interferometric gravitational wave detectors, GEO 600 does not use Fabry–Perot resonators in the arms, but instead the simplest case of an optical delay line including one folding mirror per arm. The light containing potential gravitational wave
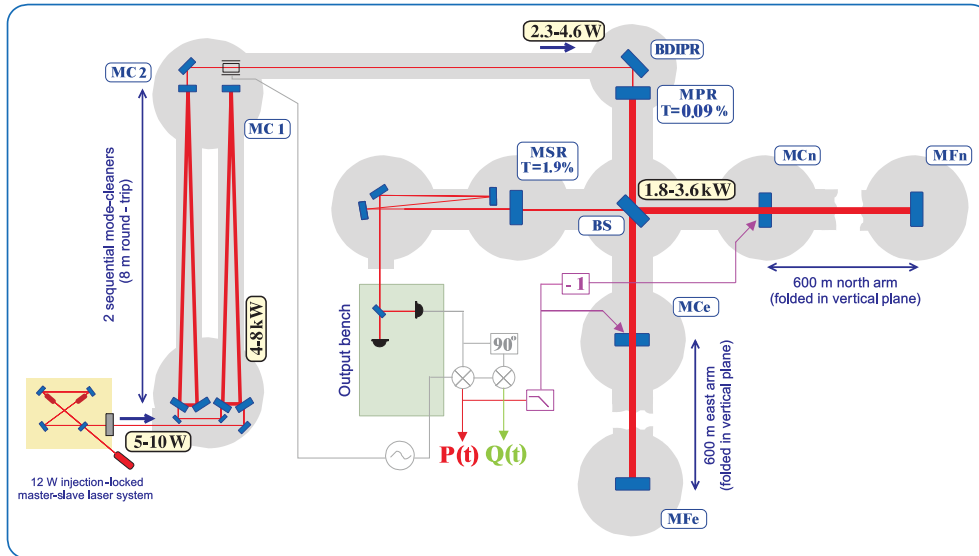
Figure 1. Simplified optical layout of GEO 600. The light of an injection-locked master-slave laser system is filtered by two sequential mode cleaners before it enters the main Michelson interferometer. GEO 600 is an interferometer with dual recycling, i.e. it uses power recycling and signal recycling simultaneously. There are no Fabry–Perot resonators in the arms, but instead the simplest case of an optical delay line including one folding mirror per arm.

information leaves the Michelson interferometer at the antisymmetric port and the signal gets enhanced by usage of a second recycling mirror, the signal-recycling mirror (MSR). The light passing the signal-recycling mirror is detected at the output bench and the gravitational wave information is derived from an RF-heterodyne method.

2. Commissioning of the GEO 600 detector

Two major changes of the detector have been realized since the end of the science run S4 in March 2005. First, the resonance condition of the signal-recycling cavity was shifted towards lower frequency in order to allow for better sensitivity in the few hundred Hz range. Second, the circulating light power was increased inside the main interferometer to decrease the influence of shot noise. Both changes improved the sensitivity of the detector and have been the last major steps towards approaching the final detector configuration.

2.1. Tuning the signal-recycling mirror to lower frequencies

GEO 600 is the first large-scale gravitational wave detector using the advanced technique of signal recycling. It allows the response of the detector to be tuned in two degrees of freedom. The reflectivity of the signal-recycling mirror determines the bandwidth of the signal enhancement, while its microscopic position, the so-called tuning, defines the frequency of maximal signal gain.

For technical reasons, we are not able to acquire lock of the detector directly at the preferred signal-recycling operating point near to its resonance condition. Instead, we acquire lock at a high detuning frequency of the signal-recycling cavity (2.2 kHz) and afterwards tune the signal-recycling mirror in small steps to its operating point. This tuning process
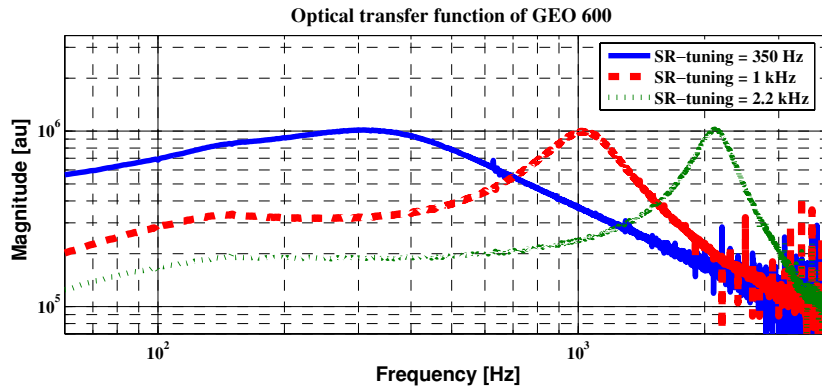
Figure 2. Optical transfer function (see the text) of GEO 600 for different tunings of the signal-recycling cavity. Lock acquisition usually takes place at a detuning of 2.2 kHz. During the science run S4 (spring 2005), GEO 600 was operated at a detuning of about 1 kHz. Since the second half of 2005, the nominal operation point of the signal-recycling mirror corresponds to a detuning of 350 Hz.

requires the simultaneous adjustment of many control parameters such as gains and phases of longitudinal and angular control systems. Up to the end of the S4 science run (spring 2005), GEO 600 had been operated at a detuning of 1 kHz. Due to a better knowledge of the downtuning parameters [5] and improvements of the Michelson angular control system, it is now possible to operate the detector at a detuning as low as 200 Hz. For sensitivity and stability reasons, a nominal operation point of 350 Hz is chosen. Figure 2 illustrates the transfer function from differential displacement to heterodyne readout, called optical transfer function, for the three cases of lock acquisition (2.2 kHz), operation in S4 (1 kHz) and the current operating point (350 Hz).

2.2. Increasing circulating light power

During the last year, the circulating light power was increased by about one order of magnitude to a light power of roughly 3.6 kW in front of the beam splitter. In May 2005, we replaced the power-recycling mirror which had a transmission of 1.35% by a mirror of higher reflectivity. The actual transmission of the currently installed MPR is 0.09% which led to an observed power-recycling factor of about 800. Due to some unexplained losses inside the interferometer, we are not yet able to establish the even higher, theoretically predicted recycling factor of 2000. The most likely suspect for the additional losses is slight beam clipping at a wrongly positioned beam dump inside the vacuum system. Further enhancement of the intracavity power was gained by using the full available laser power at the input of the first mode cleaner, which is now about 10 W.

To ease the lock acquisition of the interferometer, only half the maximal provided laser light, 5 W, is injected into the first mode cleaner leading to an optical power of 1.8 kW at the beam splitter. The attenuation of the light level is done with a remotely controlled $\lambda/2$-plate in front of mode cleaner 1. After full lock of the detector is established, the light power at the input of mode cleaner is turned up in small steps to the maximal power of 10 W. This requires a simultaneous adjustment of the gains of many control systems. The light power finally achieved amounts to about 3.6 kW in front of the beam splitter. Such high light levels can cause various problems, two of which are briefly discussed in the following subsections.

2.3. Radiation pressure compensation at the mode cleaners

At maximal input light power of 10 W, the circulating light power inside the first mode cleaner builds up to about 8 kW which, in combination with the low weight of the installed suspended mirrors (860 g), results in macroscopic radiation pressure effects. The difference of cavity length between no circulating light and the maximal intracavity power amounts to several wavelengths, more precisely to about 8.5 μm. This fact turned out to cause a problem, due to the limited range of the actuator used for the longitudinal lock of this ring cavity which in this case is the master laser piezo. The actuator was not able to follow the length change of the cavity being caused by the increasing light power shortly after acquisition. Thus, a lock could only be held for less than a second.

This problem was solved by applying a bias force to the mirrors for acquisition and then reducing this force in lock corresponding to the power build-up. Thereby, the absolute length of the mode cleaner cavity stays constant, independent of the circulating light power and radiation pressure. In order to avoid introducing additional noise, this radiation pressure compensation system is designed to apply close to zero force at final circulating light power, i.e. the nominal operating point of the mode cleaner.

2.4. Thermal effects in the main interferometer

A second potential problem of high light levels arises due to thermal effects in the optical components. In GEO 600, the thermal lensing inside the beam splitter substrate is expected to be the most critical thermal effect [6, 7]. The thermal lens in the beam splitter is assumed to be dominant over all other thermal effects such as, for instance, coating absorption and the corresponding surface deformation [8].

To evaluate the problem of thermal lensing for high intracavity power, we measured the absorption of the beam splitter. The result of this measurement was highly satisfactory. We set an upper limit for the absorption inside GEO's beam splitter substrate of less than 0.25 ppm cm^{-1}. This is the lowest value ever observed for light absorption in fused silica at 1064 nm [9]. The low absorption guarantees that even at this high power level the thermal lensing in the beam splitter will not cause significant problems. Moreover, the low beam splitter absorption will allow for further power increase in the future without the necessity of any thermal compensation.

2.5. Noise identification and reduction

One of the major tasks of the detector commissioning is the identification and elimination of technical (i.e. non-fundamental) noise in the gravitational wave channel. In GEO, we mainly use a technique called *noise projections* for identifying limiting noise sources. This method is described in detail in [10].

During the last year, a multitude of different noise sources have been identified and eliminated. As a detailed description would be beyond the scope of this paper, only a few examples of limiting noise sources that have been eliminated or reduced are mentioned:

- feedback noise from several control loops;
- phase and amplitude noise of the RF modulation;
- scattered light from various interferometer ports.

A more detailed description of the recent noise hunting effort can be found in [11].
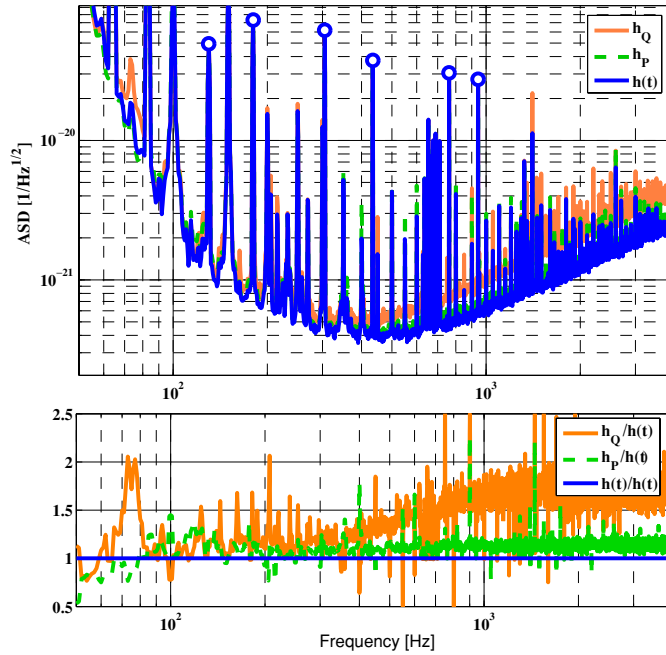
Figure 3. The $h(t)$ signal is derived by optimal combination of $h_P(t)$ and $h_Q(t)$, the two calibrated detector output signals containing gravitational wave information. Above 80 Hz, $h(t)$ is more sensitive than either $h_P(t)$ or $h_Q(t)$. A peak sensitivity of about 4×10^{-22} Hz$^{-1/2}$ is achieved. The lower plot shows the ratio of h_P, h_Q and h.

3. Calibration and detector characterization

One consequence of using signal recycling is that the gravitational wave signal gained from demodulating the light at the detector output is distributed between both quadratures (referred to as 'P' and 'Q'). Both signals are calibrated to strain using a time domain method described in [12]. The results of the calibration processes are the two signals 'h_P' and 'h_Q', both containing gravitational wave information.

3.1. Combining h_P and h_Q

After calibration, the two derived outputs h_P and h_Q contain (to within the accuracy of the calibration process) exactly the same gravitational wave information $h^*(t)$ but different noise components N_P and N_Q:

$$h_P(t) = h^*(t) + N_P(t), \tag{1}$$

$$h_Q(t) = h^*(t) + N_Q(t). \tag{2}$$

In order to get a single detector output signal, we combine h_P and h_Q using a maximum likelihood method which is described in [13]. The result of this process is an 'optimal' combination of h_P and h_Q that we call $h(t)$. Having a single signal containing gravitational wave information with maximum SNR, instead of two, eases detector commissioning, detector characterization and data analysis. Furthermore, the derived signal $h(t)$ shows at nearly all frequencies less noise than either of the two initial signals h_P and h_Q. Figure 3 shows the
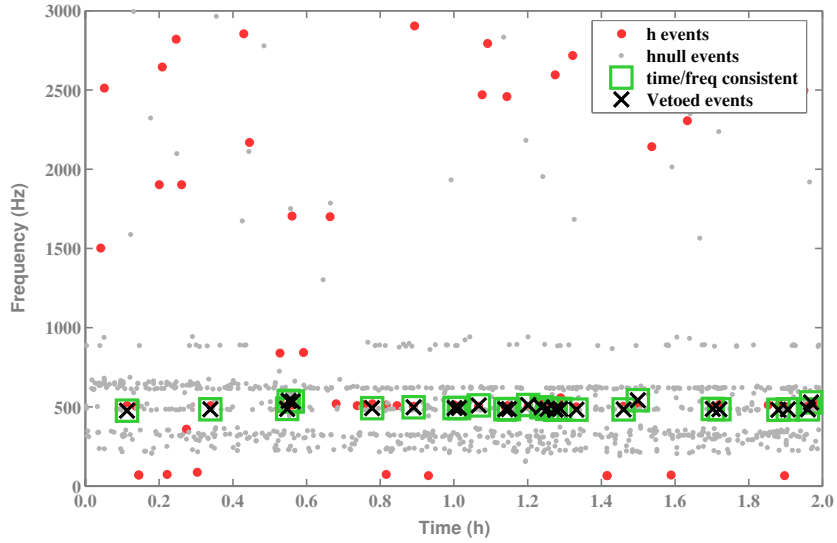
Figure 4. Application of the null stream veto to a 2 h stretch of GEO data. Detailed description of the veto method can be found in the text.

amplitude spectral density of h_Q, h_P and h and the ratio of the signals. Above 100 Hz, $h(t)$ is, on average, about 15% more sensitive than either h_P or h_Q. Only below 80 Hz does the combination not lead to an improvement in sensitivity.

3.2. Null stream veto

Besides creating a signal of maximum gravitational wave information, it can also be very useful to create a signal without any gravitational wave content. By subtraction of h_P and h_Q, a null stream signal called h_{null} is derived containing no gravitational wave information within the accuracy of the calibration:

$$h_{null}(t) = h_P(t) - h_Q(t) = N_P(t) - N_Q(t). \tag{3}$$

This signal can be used to veto (a certain class of) transient events showing up in the $h(t)$ channel [14]. In case a transient is simultaneously detected in $h(t)$ and $h_{null}(t)$, i.e. within a certain time and frequency window, an amplitude consistency test is applied. If the amplitude ratio, h/h_{null}, of a particular event is below a certain threshold, then the transient gets vetoed. Figure 4 shows the null stream analysis of a 2 h stretch of data from GEO 600. Transient events detected in $h(t)$ and $h_{null}(t)$ are marked with red and grey dots, respectively. Time and frequency consistent events are indicated by a green square. The time and frequency windows applied are 40 ms and 32 Hz, respectively. Events of an amplitude ratio not consistent to originating from a gravitational wave are vetoed (black crosses in the figure). For this particular 2 h data set, about 25% of the transients in $h(t)$ could be vetoed.

3.3. Photon pressure drive

The calibration scheme currently used at GEO 600 employs electrostatic drive (ESD) actuators to inject calibration lines, i.e. to induce differential displacement of the end mirrors (MCe and
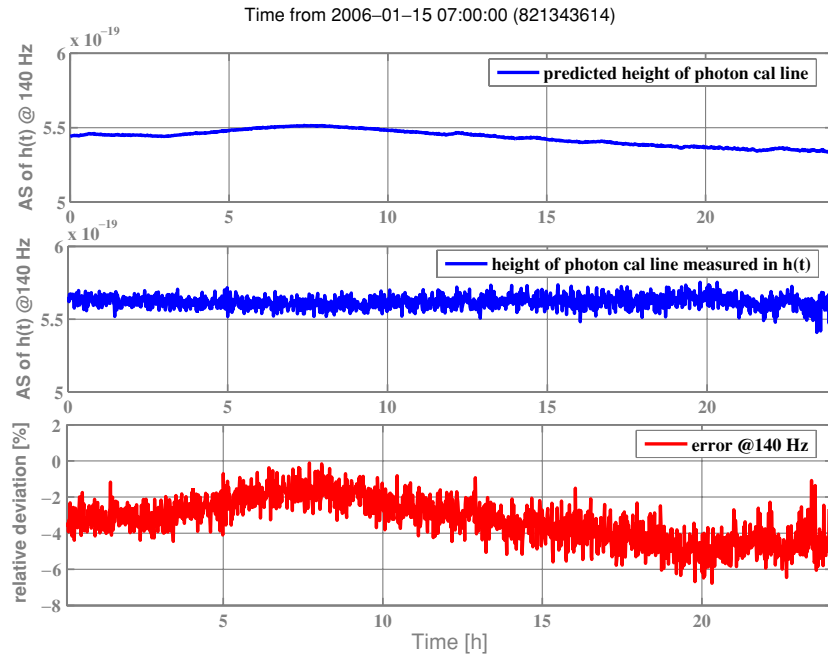
Figure 5. Performance of the photon pressure drive compared with the electrostatic drives (ESD). The first trace shows the height of a photon pressure line derived from the internal monitor of the photon pressure drive. The height of the photon pressure line measured from calibrated data (derived from the electrostatic drives) is plotted in the second trace. The relative error between ESD and photon pressure calibration is shown in the lowest subplot.

MCn). In order to check the accuracy and the long-term stability of the ESD actuators, we need an independent and long-term stable actuator that can be reliably calibrated. Radiation pressure applied by an amplitude-modulated laser shining at one of the test masses can be used for that purpose. The experimental setup of the photon pressure drive installed behind MFn (one of GEO's folding mirrors) is described in detail in [15].

Figure 5 shows the performance of the photon pressure drive over a time stretch of 24 h. The light amplitude incident on the test mass is monitored by a photodiode in the laser. Using

$$F = \frac{2\Delta P}{c},\tag{4}$$

where F is the force applied to the test mass, ΔP is the modulated light power and c is the speed of light, we can easily predict the resulting displacement of the test mass. For a modulation frequency of 140 Hz, the predicted height of a photon pressure calibration line in $h(t)$ is plotted in the top trace of figure 5. The subplot below shows the actual measured height of the calibration line in $h(t)$. The relative deviation between both calibration methods is shown in the bottom subplot. The absolute deviation between ESD and photon pressure drive is less than 7%. The relative error varies by about 4% over 24 h. The fact that the predicted height of the line in $h(t)$ shows a variation, while the measured height in $h(t)$ stays constant suggests that the change in the error is dominated by a drift in the monitor photodiode. This effect is still under investigation.
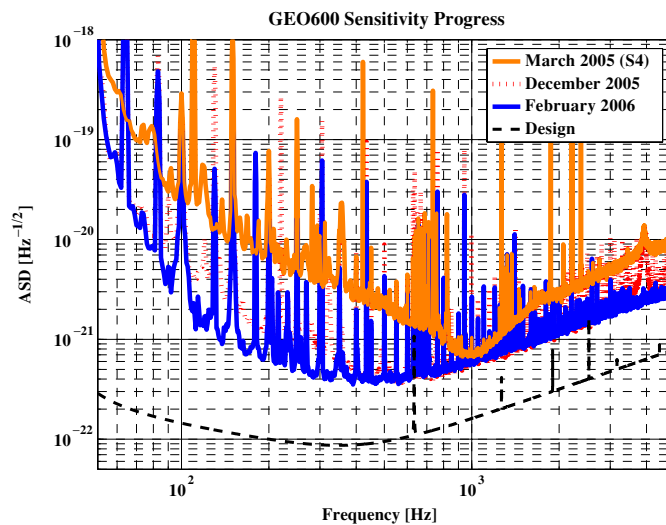
Figure 6. Sensitivity improvement of GEO 600 during one year of commissioning from March 2005 until February 2006.

4. Sensitivity improvements

Over the last 12 months, the sensitivity of GEO 600 has been improved significantly, especially at lower frequencies. Figure 6 reflects the development of the sensitivity during the last year. Between 100 and 300 Hz, a factor of about 10 was gained. The current peak sensitivity is about 4×10^{-22} Hz$^{-1/2}$ around 400 Hz. An inspiral range for neutron star–neutron star collision (optimally orientated, neutron star masses = 1.4 solar masses, SNR = 8) of 1.4 Mpc is obtained.

Acknowledgments

References

[1] Sigg D *et al* 2004 Commissioning of LIGO detectors *Class. Quantum Grav.* **21** S409–15
[2] Acemese F *et al* 2004 Status of VIRGO *Class. Quantum Grav.* **21** S385–94
[3] Takahaschi R (the TAMA Collaboration) 2004 Status of TAMA 300 *Class. Quantum Grav.* **21** S403–8
[4] Willke B *et al* 2004 Status of GEO 600 *Class. Quantum Grav.* **21** S417–23
[5] Malec M 2006 Commissioning of advanced, dual-recycled gravitational-wave detectors: simulations of complex optical systems guided by the phasor picture *PhD Thesis* Hannover
[6] Winkler W *et al* 1991 Heating by optical absorption and the performance of interferometric gravitational wave detectors *Phys. Rev.* A **44** 7022
[7] Strain K *et al* 1994 Thermal lensing in recycling interferometric gravitational wave detectors *Phys. Lett.* A **194** 124–32
[8] Winkler W *et al* The GEO 600 core optics, in preparation
[9] Hild S *et al* Measurement of a low-absorption sample of OH-reduced fused silica *Appl. Opt.* submitted

[10] Smith J R *et al* 2006 Projection of technical noise for interferometric gravitational-wave detectors *Class. Quantum Grav.* **23** 527–37

[11] Hild S *et al* 2006 Towards gravitational wave astronomy: commissioning and characterization of GEO 600 *J. Phys.: Conf. Ser.* **32** 66–73

[12] Hewitson M *et al* 2004 Principles of calibrating the dual-recycled GEO 600 *Rev. Sci. Instrum.* **75** 4702

[13] Hewitson M *et al* 2005 Optimal time-domain combination of the two calibrated output quadratures of GEO 600 *Class. Quantum Grav.* **22** 4253–61

[14] Hewitson M and Ajith P 2005 Using the null-stream of GEO 600 to veto transient events in the detector output *Class. Quantum Grav.* **22** 4903–12

[15] Mossavi K *et al* 2006 A photon pressure calibrator for the GEO 600 gravitational wave detector *Phys. Lett. A* **353** 1–3